



ELSEVIER

Journal of Nuclear Materials 266–269 (1999) 330–336

Journal of  
nuclear  
materials

EURATOM

## Simulation of helium exhaust in JET and ITER

M. Fichtmüller<sup>\*</sup>, G. Corrigan, L. Lauro-Taroni, R. Simonini, J. Spence,  
E. Springmann, A. Taroni

*JET Joint Undertaking, Data Analysis and Modeling Unit, Abingdon, Oxfordshire OX14 3EA, UK*

---

### Abstract

The problem of helium exhaust is studied using the integrated code package Combined Code Numerical Utility for Tokamaks (COCONUT): the 2D scrape-off layer code EDGE2D/NIMBUS is coupled with the 11/2D plasma transport codes JETTO and SANCO to allow consistent modelling of the entire plasma cross section. The code is first benchmarked against JET experiments in order to determine the radial helium transport in the core and in the SOL. The findings are then applied in predictive modelling of the ITER design. The results of the simulations are expressed in terms of confinement times and enrichment. For JET, we obtain values consistent with direct experimental measurements. The predictions for ITER are seen to be very sensitive to the model assumptions for the scrape-off layer. © 1999 JET Joint Undertaking, published by Elsevier Science B.V. All rights reserved.

*Keywords:* Helium exhaust; 2D modelling; Anomalous transport

---

### 1. Introduction

Sufficient helium exhaust is a vital requirement for any burning reactor. To avoid the fusion reactions being choked by excessive impurity accumulation, the helium removal rate from the divertor has to equal the production rate for an acceptable helium concentration in the core. The study of helium exhaust has traditionally been divided into the investigation of helium transport in the core on one hand and of the removal efficiency in the divertor on the other hand. However, this division conflicts with the global nature of the helium exhaust and is reflected by the relevant figures of merit. The enrichment compares the helium concentration in the divertor region to that in the core. The global confinement time combines the effects of core particle confinement time and recycling in the divertor [1,2]. Modelling efforts thus have to cover both core and edge; therefore, we make use of the global code Combined Code Numerical Utility for Tokamaks (COCONUT) (Section 2). The simulation of helium puffs in ELMy H-modes at

JET is described in Section 3. Section 4 contains results of predictive modelling of ITER.

### 2. The codes

The core codes JETTO and SANCO have been coupled with the 2D scrape-off layer code EDGE2D/NIMBUS [3] to provide an integrated global code which has been named COCONUT. The coupled code was presented in [4,5] and has now been extended to accommodate multi impurity species and to allow fully predictive simulations. The complete coupling eliminates the boundary conditions at the core-edge interface for both edge and core codes which is particularly important for time-dependent situations.

A great advantage of COCONUT is its flexibility. Depending on the problem under consideration, any part of the system can be switched off or 'frozen'. Furthermore, core and the edge can be evolved on different time scales. This point is crucial for ITER simulations where the core equilibration time is of the order of tens of seconds as opposed to the characteristic SOL time of about 50 ms. The code can then be used in a 'partially coupled' mode where the core codes are run stand-alone

---

<sup>\*</sup> Corresponding author. Tel.: +44 1235 528 822; fax: +44 1235 464 465; e-mail: mficht@jet.uk.

for specified time intervals. Between these intervals, short periods of fully coupled running ensure consistency with the SOL parameters.

A 21 moment description of the parallel transport in the scrape-off layer ensures the consistent treatment of multi impurity species of arbitrary concentrations [6]. A charge state averaged momentum equation has been developed on the basis of this model in order to reduce the computational load [7]. In addition, the use of averaged momentum equations greatly improves the stability of the impurity equations.

### 3. Helium puff experiments at JET

An overview of helium puff experiments recently carried out at JET is given in Ref. [8]. Here, we concentrate on the analysis of two ELMy H-mode experiments with type I ELMs. One shot (#33994) in the MkI divertor configuration is used to benchmark the code. A second shot (#44338) at the beginning of 1998 in the MkII divertor was selected to investigate the effects of different divertor configurations.

As a prelude to global COCONUT simulations, a study with the stand alone versions of the codes has been carried out to deduce the radial core transport coefficients (SANCO) and a base case for the divertor plasma (EDGE2D). The temperatures and the electron density in the core are not simulated here but taken from experimental measurements.

#### 3.1. Edge

A series of EDGE2D/NIMBUS stand alone runs has been carried out not only to prepare COCONUT simulations but also to identify trends in the way the divertor influences the helium exhaust. The simulations refer to the quasi steady state period between ELMs and include deuterium, carbon, and helium. The modelling of carbon is essential to obtain more realistic temperature profiles. A second reason is friction between carbon and helium which tends to drag helium out of the divertor, due to flow reversal of carbon close to the target plates. The anomalous radial diffusion and the pinch velocity of the main ions are found matching the profiles of the ion saturation current and the electron temperature at the targets as measured by Langmuir probes. The standard settings are  $\chi_i = 0.4 \text{ m}^2/\text{s}$ ,  $\chi_e = 0.2 \text{ m}^2/\text{s}$ ,  $D = 0.1 \text{ m}^2/\text{s}$  and a constant  $v_{\text{pinch}} = 9.5 \text{ m/s}$  in the scrape-off layer. The anomalous diffusion coefficients are assumed constant in flux space, i.e. increasing with flux expansion in real space. The carbon content is controlled by a constant sputtering coefficient. The measured  $\text{C}^{2+}$  photon fluxes are seen to require a sputtering coefficient of  $Y_C \geq 0.03$  in combination with a low pinch velocity for carbon of 1.5 m/s. The input power and the up-

stream density of main ions are adjusted so as to reproduce the measured deuterium photon fluxes in the divertor and the magnitude of the Langmuir probe measurements.

The results of these simulations are expressed in terms of enrichment which is here defined as

$$\eta = (n_{\text{He}}/2n_{\text{D}_2})_{\text{pump}}/(n_{\text{He}}/n_{\text{D}})_{\text{core}}.$$

The core concentration of helium is taken from experimental measurements by active charge exchange spectroscopy (CXRS). The grid of EDGE2D covered the two outermost lines of sight of the CXRS which fixed the upstream helium density in the simulation. The neutral helium concentration at the pump is computed by the Monte Carlo code NIMBUS. Direct measurements of the partial pressures at the pump were not available in MkI, but a further constraint is imposed by the helium photon flux measurements in the divertor. These could be reproduced simultaneously with those of carbon and deuterium, but only if the helium pinch velocity in the SOL was reduced to about 0.5 m/s.

The enrichment determined in this way is  $\eta = 0.08$  for #33994 in MkI and  $\eta = 0.07$  for shot #44338 in MkII. The similarity is surprising for several reasons. MkI was much more open than MkII, the MkI shot was on horizontal targets as opposed to shot #44338 on vertical targets and, finally, helium was pumped in the MkI experiment but not in the MkII shot. In a series of predictive simulations only one feature was changed at a time.

(1) Changing from MkI to MkII does increase the neutral pressure in the divertor due to the increased closure to neutrals. However, the enrichment is seen to be affected very little. The enrichment changes with other plasma characteristics which did not vary much between the two shots. For example, if the net input power is decreased in the simulations and the conditions move from high recycling regimes towards detachment, then the enrichment is seen to increase.

(2) Switching off pumping of helium in the simulations increases the enrichment by a factor of two because the differential pumping removes only deuterium from the pump volume while helium is left to accumulate.

(3) Changing target configuration from horizontal to vertical targets in JET decreases the enrichment. The reason is that the helium density is found to peak in the SOL in the inner divertor (Fig. 1). The pump ducts are located in the bottom corner of the divertor. Thus, for horizontal targets the helium peak is in direct contact with the pump while it is shielded by the private region on the vertical target. Moving to the vertical target configuration shows a decrease of the enrichment by 50% when the separatrix is still close to the openings of the pump duct. Moving the X-point a couple of centi-

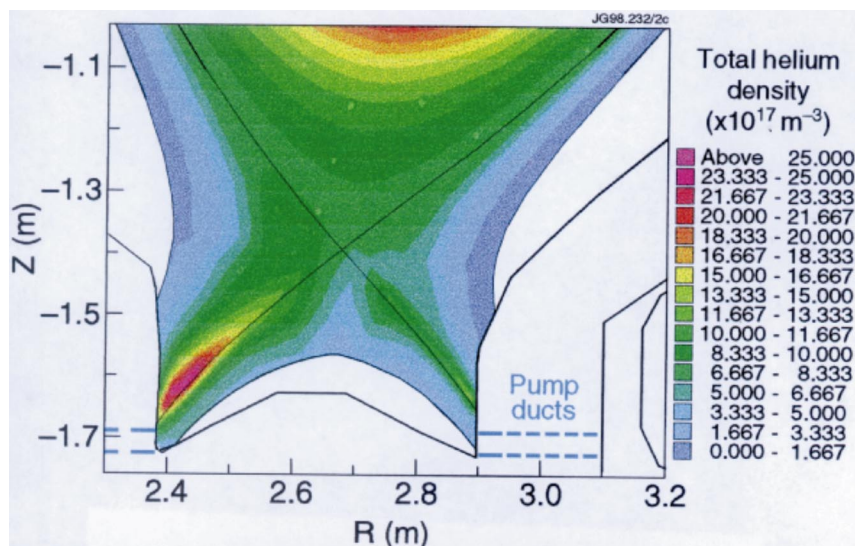


Fig. 1. Modelled helium density in #44338.

meters higher up to obtain the configuration shot #44338 causes another reduction of 20%.

Experimental determination of the enrichment was possible in the MkII campaign due to the installation of a species discriminating Penning gauge diagnostic in the pump void [9]. The ratio of the partial pressures of helium and deuterium is compared to the helium concentration in the core resulting in  $\eta = 0.08 \pm 0.04$ , well in agreement with the simulation. However, it has to be emphasised that the Penning gauge measurements do not resolve the ELMs but are ELM-averaged. The agreement holds thus only in as much as the ELM activity does not affect the helium concentration at the pump beyond the effect on the upstream concentration which is adjusted in the simulation to the ELM-averaged CXRS measurements. Furthermore, the stated value is the incremental value of the puffed helium. The face value can be as high as  $\eta = 0.2$ .

### 3.2. Core

The transport analysis in the core leads to the deduction of a set of radial transport coefficients from the radial density profiles of the impurities in shot #33994. In a source free steady state, the profile shapes yield information about the ratio of the pinch velocity to the anomalous diffusion coefficient as a function of the radius. This is a simple consequence of the ansatz  $\Gamma = D\nabla_n + nv_{\text{pinch}}$ . In time-dependent experiments like short puffs of helium, the evolution of the profile shapes depends on the speed of transport. This allows the determination of the magnitudes of  $v_{\text{pinch}}$  and  $D$ . The SANCO code calculates the impurity profiles for a given

set of transport coefficients so that the latter are in practice the result of an iterative process. The exact time dependence of the helium source is not well known since the pressure drop at the gas valve gives only a rough estimate of the actual time evolution of the puff arriving at the plasma boundary. However, the time evolution of the total helium content is a tough constraint on the specification of the puff. The boundary condition at the separatrix was chosen to be a fixed exit velocity which would balance the influx of neutrals in the steady state before the puff. The profile evolution could be tracked very closely and Fig. 2 shows the resulting transport coefficients for helium as a function of  $\rho = r/a$ .

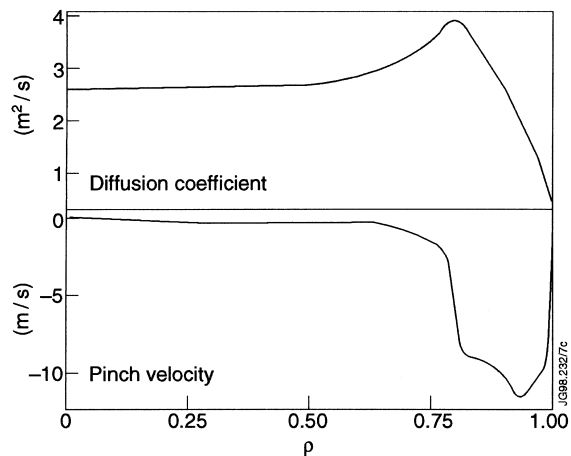


Fig. 2. Helium transport coefficients from #33994 as a function of  $\rho = r/a$ .

### 3.3. Global simulation

Finally, EDGE2D/NIMBUS and SANCO are combined in a COCONUT simulation. The code JETTO is run interpretively, i.e. the relevant profiles were taken from the experiment. The fact that the helium exhaust is an ELM-averaged process has now to be taken into account in the setup of EDGE2D which so far only addressed the phase between ELMs. The ELMs are assumed to effectively increase the radial diffusion of helium to  $D = 0.45 \text{ m}^2/\text{s}$  in the SOL. An immediate effect of the use of COCONUT was to bring the helium density at the core-edge interface up to the level measured by CXRS where the boundary condition imposed in the SANCO simulations had yielded too low densities. Fig. 3 shows the time evolution of the puff and of the total helium density from the experiment and the simulation. The experimental time trace of the helium puff is a centered Gaussian to represent the measured integral puff. The decay of the helium density is due to the helium pumping by a layer of argon frost on the cryo pump.

A problem is apparent in the difference of the amount of helium puffed in the experiment and the simulation. The radial profiles correspond to considerably more helium than was released by the gas valve. On the other hand, the helium photon fluxes in the divertor region as computed by the COCONUT simulation are too high. If the helium puff is halved in the modelling to yield a total content slightly below the actually injected helium, the divertor fluxes agree well (Fig. 4). The simulation has

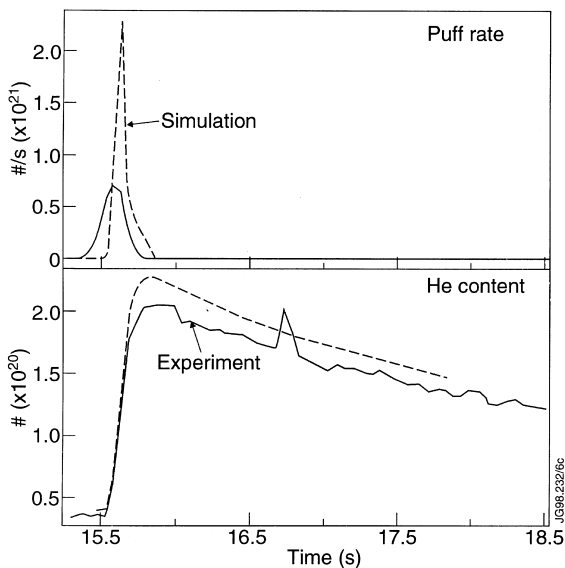


Fig. 3. Time evolution of helium puff and helium core content in shot #33994 and in the simulation.

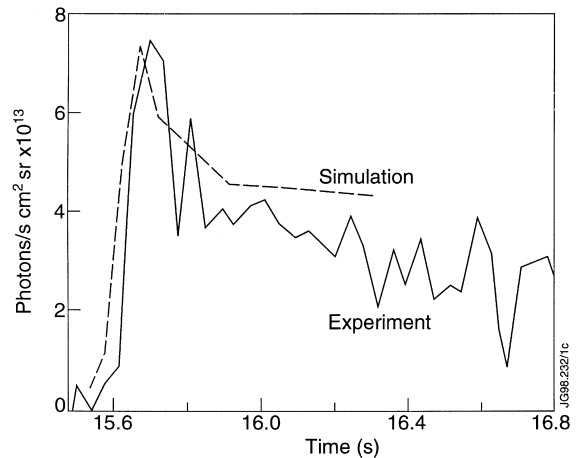


Fig. 4. Experimental and modelled helium photon flux in the outer divertor.

been stopped at 16.3 s to save computing time. The previous simulations had already shown that the continuous decrease of the photon flux at later times is reproduced as well.

The global helium confinement time  $\tau_x^*$  [1] can be obtained by fitting an exponential function to the experimentally observed decay rate which is well reproduced in the simulation. For shot #33994, we obtain  $\tau_x^* = 4.5 \text{ s}$ . This confinement time can be expressed as  $\tau_x^* = \tau_x / (1 - R_{\text{eff}})$ . The global or 'effective' recycling coefficient contains the overall effect of the pumping efficiency, the recycling in the divertor and the back penetration of helium into the core. The particle confinement time  $\tau_x$  is the characteristic time for a particle to leave the core plasma. Switching off any recycling of helium at the target plates and the walls,  $\tau_x$  can be obtained directly in the simulation. The simulation with  $R_{\text{eff}} = 0$  results in a fast decay with an e-folding time of  $\tau_x = 0.2 \text{ s}$ . With this particle confinement time, it follows that  $R_{\text{eff}} = 0.96$ .

## 4. Helium exhaust in ITER

The simulations of ITER have been carried out using the vessel data and magnetic configuration of the ITER EDA design as from end 1997. It is assumed first that the JET results concerning the particle transport can be transferred to ITER without changes. Of course, this need not to be true and, in one instance, it is actually not compatible with the ITER design. In this case we choose the simplest possible scaling, but otherwise we use the JET H-mode scenario throughout. For comparison, a different set of transport coefficients and other input parameters will also be used.

#### 4.1. Edge

The input power across the core boundary is set to 200 MW corresponding to about 300 MW fusion power and 100 MW radiation losses in the core. The separatrix density of the main ions is fixed at  $2.0 \times 10^{19} \text{ m}^{-3}$ . This amounts to 15% of the projected central density in ITER which is the typical percentage used in simulations of JET discharges. All coefficients for the radial transport are set identical to those used in the JET simulations. The helium content is prescribed so as to obtain separatrix densities of 10%–15% of the main ion density. Carbon is again introduced via a fixed sputtering coefficient of 3%. This leads to about 110 MW of carbon line radiation in the divertor. Further 30 MW are lost due to ionisation and molecule dissociation of deuterium and other small contributions. The remaining 60 MW are fairly evenly split between inner and outer target with the peak power loads not exceeding  $7 \text{ MW/m}^2$ , compatible with the design limit of  $10 \text{ MW/m}^2$  [10]. However,  $Z_{\text{eff}}$  rises to 2.6 at the core boundary 2 cm inside the separatrix. Both inner and outer target are attached with target separatrix densities of  $1.5 \times 10^{21} \text{ m}^{-3}$ . In Fig. 5, it can be seen that the helium peaks in the private region confirming the positioning of the pump ducts (the pump is modelled by prescribing a transparency of 0.006 at the pump surface corresponding to a pumping speed of  $200 \text{ m}^3/\text{s}$ ). The attached conditions are unfavourable for the enrichment which is in this simulation 0.07 (design requirement of 0.2). The enrichment is evaluated under the assumption that the helium concentration is constant throughout the core as found in the core modelling described below.

Simulations of an alternative scenario as proposed by Kukushkin et al. [11] were performed in order to assess the uncertainties in the code predictions. The input parameters are in this setup  $P_{\text{input}} = 200 \text{ MW}$ ,  $n_{\text{sep}} = 3.0 \times 10^{19} \text{ m}^{-3}$ ,  $Y_C = 0.01$ ,  $\chi_i = 1.0 \text{ m}^2/\text{s}$ ,  $\chi_e = 1.0 \text{ m}^2/\text{s}$ ,  $D = 0.3 \text{ m}^2/\text{s}$  and no particle pinch velocity. Here, the diffusivities are assumed to be constant in real space. The plasma solution is substantially different. The inner target is completely and the outer target partially detached. The outer target receives the entire power load of 60 MW, but due to a much wider density profile the peak power load is again  $7 \text{ MW/m}^2$ .  $Z_{\text{eff}}$  drops to 1.6 at the boundary. These findings are consistent with the results in Ref. [11] and favourable for ITER. The enrichment is  $\eta = 0.9$  which is a drastic increase with respect to the results obtained with the JET-based set of input parameters.

#### 4.2. Core

The aim was to obtain an ignited base case where the fusion reactions provide a central helium source. The boundary conditions  $n_i = 3 \times 10^{19} \text{ m}^{-3}$ ,  $T_e = T_i = 1.2 \text{ keV}$  and  $n_{\text{He}} = n_C = 3 \times 10^{18} \text{ m}^{-3}$  were taken from EDGE2D results. Combined JETTO/SANCO runs showed that rather generous assumptions were necessary in order to achieve ignition in such circumstances. In JET, the carbon profiles are seen to be flat or even hollow [12]. The carbon transport was therefore assumed to be purely diffusive, leading to a flat carbon profile in the core. The deuterium transport was chosen to include a pinch resulting in central densities of  $1.4 \times 10^{20} \text{ m}^{-3}$  and a central  $Z_{\text{eff}}$  of 1.8. The helium diffusivity

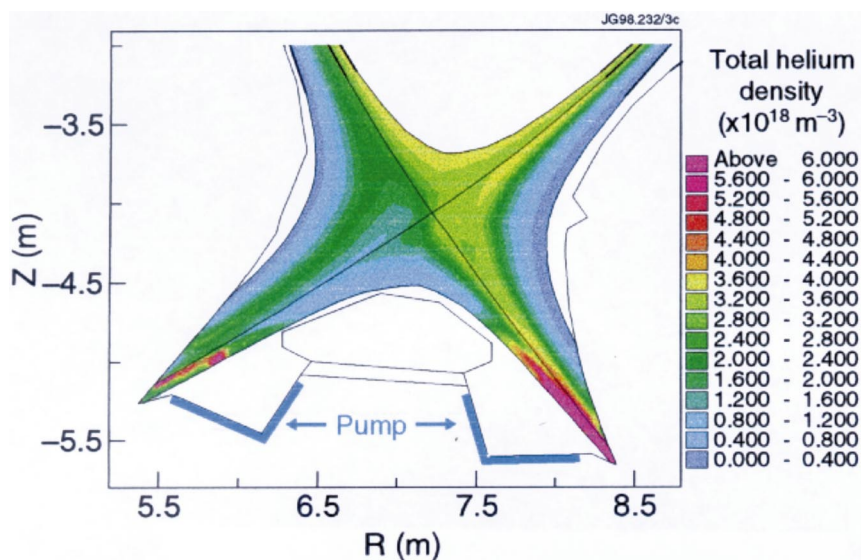


Fig. 5. Modelled helium density distribution in ITER.

was taken from #33994, but the pinch found in that shot had to be scaled down with the minor radius. While this scaling has little theoretical foundation, it is often used and certainly necessary to avoid excessive helium densities in the core. The thermal diffusivities are calculated in JETTO from a non-local mixed Bohm/Gyro-Bohm model developed at JET [13]. Sawtooth activity is taken into account by strongly increasing all radial diffusivities in the central region. Ignition was only achieved with a narrow edge transport barrier of 5 cm in which the coefficients are reduced to the low scrape-off layer values.

#### 4.3. Global simulation

Global simulations of ITER in which all variables are evolved are under way. Here, the more modest goal is the determination of the helium confinement times which are carried out with a frozen background plasma. For a burning plasma, the expression for the global confinement time is changed to  $\tau_z^* = \tau_{z1} + R_{\text{eff}}\tau_{z2}/(1 - R_{\text{eff}})$  where  $\tau_{z1}$  is the time it takes for a fusion produced alpha particle to leave the plasma for the first time and  $\tau_{z2}$  refers to particles that have been recycled at least once. To distinguish between the two particle confinement times  $\tau_{z1}$  and  $\tau_{z2}$ , SANCO is first run stand alone to obtain particular initial profiles of the helium density. In one case, the reaction rate was artificially enhanced by a factor of five and the boundary density reduced to  $3.0 \times 10^{17}$ . This ensures that the profile is representative of the distribution of first time passing alpha particles. In the subsequent COCONUT run, the wall recycling is switched off which excludes any contribution by recycled particles. During the run, 20 ms of fully coupled computations are followed by 200 ms in which only the core is evolved. With a frozen background plasma, 20 ms is seen long enough for the scrape-off layer to establish a new equilibrium between the influxes from the core and the outfluxes at the target plates. The decay of the initial helium content is shown in Fig. 6 corresponding to a confinement time of  $\tau_{z1} = 1.9$  s. To determine  $\tau_{z2}$ , the

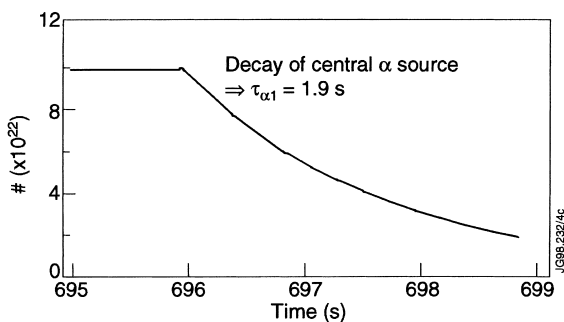


Fig. 6. Simulated decay of the helium content in ITER for zero helium recycling.

initial profile is calculated without any central source and we obtain  $\tau_{z2} = 1.8$  s, only slightly lower than  $\tau_{z1}$ . Neutral fuelling from the edge does not play a role since the scrape-off layer is completely opaque to neutrals. The similarity of the two transport times in spite of very different initial profiles is due to the volume effect: the difference in the sources shifts the bulk of the helium content by only 25 cm. Although these particle confinement times are even shorter than the expected energy confinement time of about 4 s, the helium exhaust in these simulations, where we used the JET H mode scenario, is fairly poor due to insufficient pumping. The global confinement time which is determined by the pumping speed is obtained from a simulation in which the helium diffusivity in the SOL is raised to  $D_{\text{He}} = 0.45$  m<sup>2</sup>/s (see JET simulations). This results in  $\tau_z^* = 81$  s and a global recycling coefficient of  $R_{\text{eff}} = 0.98$ .

#### 4.4. Discussion

Probably the least understood process involved in transport modelling is the radial particle transport. Predictive modelling as for ITER is therefore prone to uncertainties stemming from lack of reliable scaling laws for the anomalous particle transport. A common approach in such situations is the one of sensitivity studies and this is what has been attempted here. Two sets of input parameters originating from different points of departure, the H-mode scenario from a naive no-scaling perspective and the scenario of [11] from compatibility considerations, have been seen to yield very different results for the scrape-off layer conditions. This shows that even if we are in the position to perform global simulations which reproduce experimental findings and which can in principle be used for predictive purposes, the current uncertainty of transport models prevents conclusive answers.

### 5. Conclusion

The analysis of helium puff experiments at JET with both EDGE2D/NIMBUS and COCONUT was able to reproduce the experimental findings concerning the time evolution and the enrichment. Some trends for the enrichment were identified. The use of COCONUT has shown that it can provide a consistency check on experimental data. Simulations of ITER using the input parameters determined from JET resulted in an enrichment for ITER of 0.07. This was reflected in time-dependent simulations where a high global recycling coefficient of 0.98 prevented a rapid helium exhaust in spite of otherwise short particle confinement times. However, comparison with a different set of input parameters showed a strong sensitivity of the helium exhaust on the radial transport in the scrape-off layer. It

has to be noted that the same sensitivity holds for the core transport, although it has not been the focus of this work.

### Acknowledgements

We wish to thank J. Ehrenberg, M. Groth, M. v. Hellermann, R. Monk, M. Stamp and G. Vlases for helpful discussions and the contribution with experimental data.

### References

- [1] D. Reiter et al., *Nucl. Fusion* 30 (1990) 2141.
- [2] J. Hogan, *J. Nucl. Mater.* 241–243 (1997) 68.
- [3] R. Simonini et al., *Contrib. Plasma Phys.* 34 (1994) 368.
- [4] A. Taroni, The JET Team, *Proceedings of the 16th IAEA Fusion Energy Conference, IAEA-CN-64/D3-3*, Montreal, Canada, 1996.
- [5] L. Lauro-Taroni et al., *Contrib. Plasma Phys.* 38 (1998) 242.
- [6] M. Fichtmüller, G.J. Radford, *JET Report JET-R(97)05*, 1997.
- [7] M. Fichtmüller et al., *Contrib. Plasma Phys.* 38 (1998) 284.
- [8] M. Groth et al., presented at 25th EPS, Prague, Czech Republic.
- [9] D. Hillis et al., *Fusion Eng. Design* 34–35 (1997) 347.
- [10] DDD 1.7, ITER Final Design Report, 1998.
- [11] A. Kukushbin et al., *Contrib. Plasma Phys.* 38 (1998) 20.
- [12] M. v. Hellermann et al., 22nd EPS Conference, vol. 19C, Part II, 1995, p. 9.
- [13] M. Erba et al., *Plasma Phys. Control. Fusion* 39 (1997) 261.